Journal of Information Technology Management

Print ISSN: 2008-5893

Online ISSN: 2423-5059

Real-Time Deep Intelligence Analysis and Visualization of COVID-19 Using FCNN Mechanism

Cherukuri Triveni*

*Corresponding author, Department of Computer Science and Engineering, Velagapudi Ramakrishna Siddhartha Engineering College, Vijayawada, India. Email: cherukuri.triveni1357@gmail.com

K. Suvarna Vani

Department of Computer Science and Engineering, Velagapudi Ramakrishna Siddhartha Engineering College, Vijayawada, India. Email: suvarnavanik@vrsiddhartha.ac.in

M. Likhitha

Department of Computer Science and Engineering, Velagapudi Ramakrishna Siddhartha Engineering College, Vijayawada, India. Email: likhithamorla9@gmail.com

Abstract

The Analytic visualization suggests representing knowledge during a visual type that may be charts, graphs, lists, or maps. The COVID 19 detection and analysis of spreading is very important for countries. Database management with respect to virus deep analysis is a critical task to the researcher through conventional algorithms. The RNA, DNA, and biological data are helping to the bio-inspired algorithm but its implementation can be complex by software tools. Therefore, an effective technique is required to cross over the above limitations. So that covid 19 pandemic data analysis is performed through FCNN (Fully conventional Neural Network) pre-training network. The dataset is collected from social media, Kaggle, and GitHub databases. At 1st stage, the auto stack encoding process is applied later same data is processed with FCNN deep learning classifier. In this research work, covid-pandemic affects parameters like infected persons, deaths, active cases, and recovering cases. The FCNN is take care of feature extraction, training, testing, and classification. Finally using a confusion matrix accuracy of 98.34%, sensitivity 97.63%, Recall 98.26%, and F measure 98.83% had been estimated.

Keywords: DNA RNA sequence, COVID-19, SARS-COV-2, Coronavirus, Pandemic.

Journal of Information Technology Management, 2023, Vol. 15, Special Issue, pp. 102-119
Published by University of Tehran, Faculty of Management
doi: https://doi.org/ 10.22059/jitm.2022.89414
Article Type: Research Paper

Received: February 26, 2022
Received in revised form: May 07, 2022
Accepted: August 18, 2022
Published online: October 19, 2022

Introduction

An unknown viral pneumonia outbreak occurred in Wuhan's population in December 2019. In 2019, an ICTV (International Committee on Taxonomy of Virus) officially designated Severe Acute Respiratory Syndrome Corona Virus 2 (SARS-CoV-2) as the cause of coronavirus illness 2019. (COVID19). Because of SARS-fast CoV-2's spread and high infectiousness, early screening, isolations, & treatment action for individuals caused by corona are critical. One of many coronaviruses, the Severe Acute Respiratory Syndrome Corona Virus 2 (SARS-CoV-2) virus is characterized by its single-stranded RNA genome and lack of segmentation ZZuuu P et a,,,)))))) eee n eeagggg rraee aab OORFaa)) , eee " aaaaaaaaaaa eegnnn UU,,, the spike gene (S gene), the envelope gene (E gene), the membrane gene (M gene), the ,,, ccccaddddddeee NNgeee,, eee " ,,,, , dd a rrrrrr ff nnnnnnn nnnnccceeeed eee n eeagggg frames are all found in the RNA genome (Qiang X L et al., 2020).

It is possible to undertake quantitative analysis using standard curves and real-time quantitative PCR (qRT-PCR). Fluorescent groups are included in PCR reaction systems, and the buildup of fluorescent signals is monitored in real-time. SARS-CoV-2 is diagnosed by qRT-PCR because of its high sensitivity and excellent specificity. 2–6 as of now, qRT-PCR is most often used to identify SARS-CoV-2.7–9 in throat or nose samples; other studies have also used serum or fecal or ocular secretions (Ou X et al., 2020). When analyzing SARS-CoV-2, reverse transcriptase (RT), PCR, & Taqman probes must be used. 3 In most cases, results are available within four to six hours. Due to their ability to minimize non-specific amplification, Taqman probes may reduce false-negative findings if the binding sites contain variations. Furthermore, since the targets for SARS-CoV-2 testing share similar gene segments with SARS-COV-2, FP (False Positive) findings used for further corona virus deceases are possible. This can be done by synchronizing the finding of many objective frequencies or by generating more accurate primers and probes for the virus's genetic material progression (Kailasam S et al., 2021).

A number of issues have arisen with qRT-PCR assays used for COVID-19 test, however. First and foremost, since RNA viruses are subject to mutation and recombination, the sensitivity of these tests may be reduced. Experiment settings and staff performance have a significant impact on the detection outcomes (Moore J H et al., 2020). It was stated in the clinic that a CT scan was positive but qRT-PCR results were negative. Consequently, several scientists and doctors feel that CT scan data and qRT-PCR results should be coupled to evaluate infection, therapy and outcome. Early detection, isolation, & treatment of COVID-19 are critical on this point, according to qRT-PCR tests against the virus (Alkhamis M A et al., 2020). Standardizing sample compilation, integrating multi-site and multi-species findings, tightly monitoring the excellence of reagent equipment, and enhancing laboratory excellence are all ways to increase the accuracy of SARS-CoV-2 testing in follow-up studies (Dhiman, G et al., 2021).

Portable equipment for SARSCoV-2 screening may be easily used and findings can be easily shown in this mini-review (Gerkin R C et al., 2020). For the most part, the assays described in this study use nucleic acid detection & antibody detection as their foundations. COVID-19 should be easier to diagnose with these new tests, which we hope to be published in the near future (Qiang X & Kou Z, 2019).

SARS-CoV-2 S and N proteins, for example, induce an organism's humoral immune response, which may lead to an antibody response. Early antibodies include IgM and subsequently IgA antibodies, which then progress to IgG antibodies (Guan W J et al., 2020). The concentration of IgG antibodies will continue to rise, while the concentration of IgM antibodies will go on to drop until it vanishes, and IgG antibodies will be there for a longer duration. Specific IgM & G antibodies are a pair that emerges sequentially and the alterations in both antibodies are linked (Saikumar K et al., 2022).

Due to the fact that viral load drops over the course of a week after the onset of symptoms, testing results are highly dependent on when samples are taken (Zhu N et al., 2020). Anti-IgG and anti-IgM antibodies may be detected depending on the seroconversion potential of the patient and normally appear one to two weeks after the onset of symptoms, although this might take longer in certain cases. PCR detection's sensitivity is going to be drastically degraded at this point. When COVID-19 was diagnosed by immunoassay, it was discovered that the IgG ratio grew over time from one week after symptoms began to emerge, whereas the method's susceptibility peaked and subsequently fell (Ruben J G et al., 2019). When developing COVID-19, it was discovered that IgM may be present sooner than IgG, therefore simultaneous testing of both may improve diagnosis accuracy. lateral flow assay (LFA) is a simple and rapid approach that does not need much training before it can be used. LFA's price and simplicity of use make it ideal for testing facilities with limited resources or hospital point-of-care (POC) scenarios. Half-strip LFA was used in COVID-19 detection by Grant and colleagues. An investigative casing to a wicking pad were used in the half-strip LFA, which may be used to pre-mix the sample and conjugate in a 96-well plate (Sifuentes-Rodríguez E & Palacios-Reyes D, 2020). As for the detection level, it stood at 0.65 ng/mL. More than 18 days after the beginning of the initial symptoms or in no symptoms patients, IgG antibody testing is particularly useful. It's not clear whether assessing IgA or M is similarly effective, but their findings suggest that doing so might lead to more false-positive outcomes without considerably enhancing diagnostic performance (Kouser, R.R et al., 2018). A total of 92.1 percent of all LFAs were able to identify IgG antibodies 14-25 days following the start of symptoms, but an IgG ELISA could only detect 89.5 percent. The sensitivity of LFAs for the detection of IgG antibodies was reported to be > 92.00 percent on 2–3 weeks after the first symptoms, whereas the sensitivity of ELISAs was 89.5 percent for the detection of IgG (Qian Z et al., 2015).

Electrochemical detection: Biosensors with high sensitivity, cheap cost, simplicity of use, and robustness may be used in clinical diagnostics since they have these properties. It is

expected that electrochemical biosensors will play an essential role in clinical diagnostics & point-of-care (POC) recognition in the future. For nucleic acidic biosensors, super sandwich-type electrochemical biosensors offer a lot of promise in the diagnostic arena (Kumar K S et al., 2021).

When it comes to the electrochemical paper analysis device (ePAD), there are three different types: one that is used for the actual testing of COVID-19 and the other two that are used for countering. The S protein, which includes the RBD, is utilized to ensure that the COVID-19 antibody enters the functional ePAD examination segment. Analyze the electrochemical response using the SWV approach, which diminishes as immune complexes build. SWV. In a paper-based electrochemical technique for immunoglobulin detection, Yakoh et al. reported 100% sensitivity and 90% specificity. Data collection for epidemiological reporting & communication of test results with doctors may be smoothly integrated via telemedicine systems when mobile devices are used as testing equipment (V., Muthukumaran et al., 2021). Electrochemical detection of SARS-CoV-2 RNA utilizing calixarene-functionalized graphene oxide was developed by Zhao et al. 85.5 percent of the time with 200 copies/mL. That team created a diagnostic system called plug–and–play. The best thanks to tracking the covid-19 natural event are victimization information & visualization. COVID19 patterns are often conflicting, and when representations are accessible, this is often the case (Djomkam A L et al., 2020). Information visualization is allowing comprehension of the coronavirus epidemic with the toilet. Dashboards from Johns Hopkins University and the World Health Organization provide updates. Severe Acute Metabolic Syndrome (SAMS) has caused a widespread irruption of coronavirus in 2019.

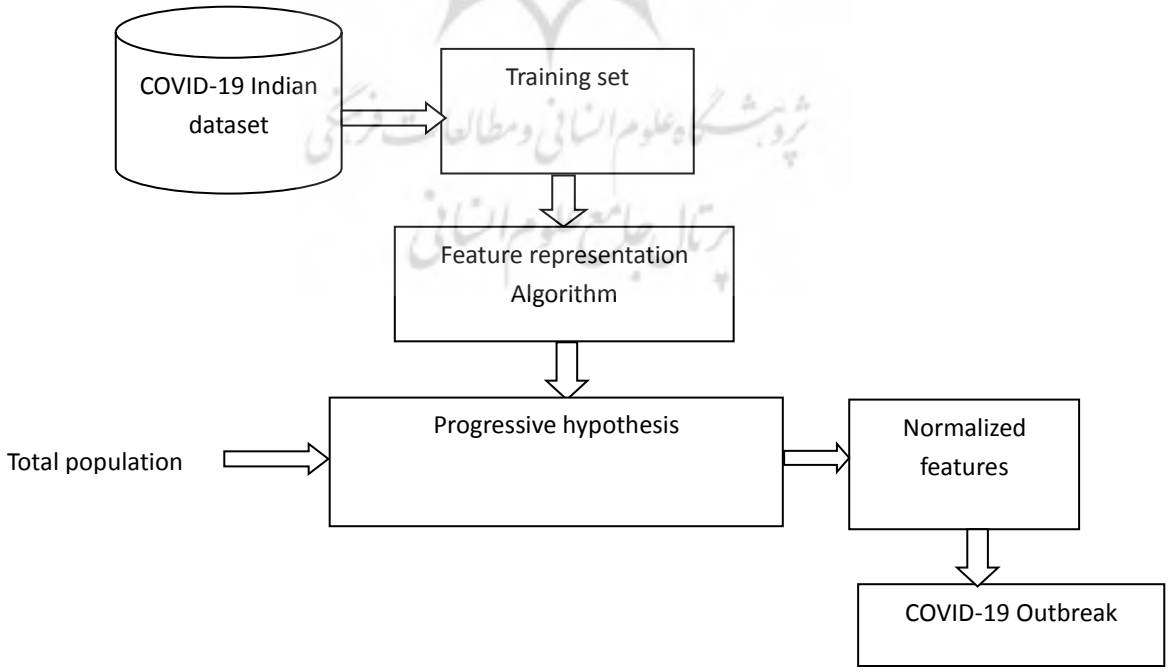

gggrr e .. Tims s. riss nnN Nll iaaar ML kkk ii ggrmm

Human populations have been devastated by Coronavirus 2. It has been an unbroken way of reporting new cases and fatalities since its inception in China's metropolitan center town. What makes it further worse is the virus's virulence and, as yet, undiscovered method figure 1. The present task of accomplishment has been sluggish to multiply due to societal distance, resulting in a hurry to provide advanced, effective diagnostic tools in addition to treatments.

By using visualizations to map the coronavirus, data scientists and researchers are cooperating. Visual image approaches are assisting the general population in comprehending COVID-19 and implementing safety measures. The John Hopkins dashboards have supplied consistent and real-time information on the coronavirus since the outbreak of COVID-19. We suggest a Progressive differential regression toward the mean (PPDLR) model and attempt coarse-grained prophetical grouping using a nonlinear international Pandemic Machine Learning (NGPML) model to overcome these issues. Throughout this investigation, I mostly used the PDR-NML technique to estimate the natural occurrence of the COVID-19 pandemic in Asian countries based on the available data (Issa N et al., 2020).

Literature Review

Su Zhao et al Proposed to predict the 3D macromolecule models of the RBD domains of the point macromolecule using similarity modelling mistreatment of the SWISS-MODEL service and to compare them to the crystal construction of the RBD domain of the spike macromolecule of the SARS-CoV. PengZhou et al proposed RNA extraction whenever business kits were used; the manufactuee'' σ eeeœiisss ee ee eeeeeeee eeeee eee .... yyggg... RNA was extracted from two hundred samples through the High Pure microorganism polymer kit (Roche). Gang Fang et al the coronavirus transmission phenotype was discovered.

Predictors like this one use feature descriptors including configurational and position-specific properties to identify key aspects of viral proteins. Xiuyuan Ou et al That we have a tendency to incontestible that SARS-CoV-2 cells is especially mediate through endocytosis which, cathepsin L area unit important for virus entry. M.A. Nasser Hajibagheri et al To generate hydrophobic and positively charged nucleic acid carbon coated grids that are adhered to the surfaces, a variety of treatment approaches are available. Jason H. Moore et al Researchers in the five disciplines of medicinal IP have the potential to make significant contributions to solving these problems, according to the authors. Chong Li et al Molecular forensics has shown to be an excellent technique for tracing the evolutionary history of many animals and human illnesses. Feng Shi et al proposed to discuss, however, AI provides safe, correct and, economical imaging solutions in COVID-19 applications.

They devised an optical detection method for SARS-CoV-2 testing that was based on LAMP and CRISPR/Cas12a technology and was free of contamination; the whole procedure took about forty minutes and produced twenty replicas (100 percent positive and negative agreement). The RT-LAMP reagent was introduced towards the test tube after the RNA had been isolated from respiratory pharyngeal swabs using an RNA extraction kit. Volatilization

of the different solutions was avoided by adding mineral oil to the RT-LAMP reagent afterwards. CRISPR and Cas12a reagents were added to the tube cap prior to isothermal conditions for RT-LAMP. Rather of opening the tube cap and allowing reagent to leak out, it was reopened and reagent was added. This prevented the risk of reagent aerosol contamination that may have occurred if the tube cap had been opened. Once the 3D printer has finished printing the tube, the fluorescence signal may be seen using simply a smartphone (Kumar, V. V et al.,2021) . In less than 40 minutes, the full amplification and detection process may be completed. SARS-CoV-2 was successfully detected using this technique, which does not react with other prevalent viruses.

RT-LAMP and CRISPR-Cas12a systems were used in a simple activation system with five copies by Wang et al. in their "opvCRISPR" visual testing approach for SARS-CoV-2. SARS-CoV-2-RNA obtained from swab samples was put to the bottom of the tube, and CRISPR/Cas12a was placed on top of it. For this approach, you just need a few simple supplies: pipettes, reagent tubes, block heaters, and blue light bulbs. A carrying case of 60–50 cm2 may hold all of the gear. The LAMP amplifier cleavage of CRISPR-Cas12a resulted in a fold up enhance in finding compassion. Fluorescence detection was used in this approach, which was simpler to discern than the colorimetric method, which relied on the naked eye.

Both the Cas13 and Cas12a-based DETECTR32 and SHERLOCK (Specific High Sensitivity Enzymatic Reporter Unlocking)32 systems use Cas13 and Cas12a. After being directed by crRNA, Cas13 is capable of bond to the object succession in order to create an inactive nuclease-inactivated complex (RNP). When it binds to a matching RNA, RNP cleaves all nearby single-stranded RNAs (ssRNAs) without discrimination. To disclose the target sequence, Cas13 is activated and cuts fluorescent RNA that can be quenched, producing a measurable signal. Recombinase polymerase augmentation (RPA) or RT-RPA reagents were used to boost the sensitivity of the extracted DNA or RNA. The "SHERLOCK" approach involves combining RPA with T7 transcript to convert DNA into RNA for further Cas13 testing. SARS-CoV-2 was recently detected using this method, and it was further developed as "SHINE36" for the identification of specimens without the need for genetic amplification.

SARS-COV-2 was diagnosed using CRISPR-Cas13a too a Smartphone camera in a study by Fozouni et al., who found that the virus could be detected directly from nasal swab RNA. A sensitivity of 100 copies/L may be achieved in 30 minutes using this approach (Figure 1C). Enhanced sensitivity and specificity by combining SARS-CoV-2-targeting crRNAs with direct viral load detection. Smartphone-integrated assay allows for quick, low-cost POC screening of SARS-CoV-2 at a low cost. The authors used a modest, low-cost laser lighting and optical collecting device to show the mobility and simplicity of their technique. The smartphone camera's great sensitivity and wireless connection make it a potentially useful tool for the diagnosis of POC diseases in locations with limited resources. Broughton et al. have demonstrated that Cas12 can be used to identify specific coronavirus sequences for the

detection of SARS-CoV-2 using a DETECTR-based technique (10 copies per response). It exhibited a 95% positive predictive value and a 100% negative predictive value. "All-In-One-Dual CRISPR-Cas12a (AIOD CRISPR)" is a revolutionary optical testing instrument that may be used at home or in clinics and is speedy, convenient, and ultrasensitive. Clinical swabs from COVID19 were used to demonstrate the viability of this diagnostic method. By using only a hand warmer as an incubator, researchers were able to detect COVID-19 in less than 20 minutes and with 5 copies/L of the virus present in the blood. Pre-amplification and manipulation are necessary for most CRISPR-Cas nucleic acid assays, which significantly delays the detection process and increases the risk of contamination by transporting amplification products. As a result, there was no need to separate pre-amplifying samples or manually segregate Cas enzymes in AIOD-CRISPR analysis, which prevented the need to separate pre-amplifying samples. As a result, this approach displays its high level of specificity in detection, which may be attributable to the particular single bases of CRISPR-Cas12a.

(Syed Thouheed Ahmed et al., 2022) Tweets that included information suggesting that the user or a family member had been exposed to COVID-19 were known to us. Richard C. Gerkin et al For the duration of the research, we sought to find the best reliable prediction of COVID-19-associated fragrance restoration. Zheng Kou et al Amino alkanoic acid mutations and pandemic risk may be accurately predicted using machine learning methods with long evolutionary distances. W. Liang et al As of January 29, 2020, there were 1099 instances of Covid-19 in dry land China that had been verified in laboratories across 30 provinces, autonomous areas, and municipalities, according to our research. The initial goal of the composite finish was to be admitted to an ICU, to need mechanical ventilation, or to die.

Trevor Bedford et al Seasonal flu shots will continue to be the primary method of preventing influenza. Xiang Zhao et al We expect to report on a single CoV (2019-nCoV) found in Chinese hospitalised patients in December 2019 too the New Style calendar month of 2020. Whole-genome analysis, direct PCR, and culturing of bronchoalveolar-lavage fluid from 3 patients confirmed the existence of this virus. Geert-Jan Boons et al A total of five S genes from BCoV strain Mebus, OC43 ATCC VR-759, PHEV strain UU, HKU strain Caen1 and MHV strain A59 were analysed for their 5'-terminal sequences (GenBank: P11224.2)

Erika Sifuentes-Rodríguez et al The importance of CoVs at a public health level emerged within the twenty-first century, with the identification of 2 new kinds of beta-CoVs, SARS-CoV & MERS-CoV, which cause severe metastasis syndrome. Martino Bertoni et al SWISS-modeling MODEL's engine is its beating heart. In order to generate an association macromolecule model, it requires a guide structure and a target-template sequence alignment to be provided. Xiuyuan Ou et al fusing of the membranes is the mechanism through which this occurs. Infectious agent fusion proteins use a convoluted approach that involves a shift from the stable prefusion phase to the six-helix bundles postfusion state. Guangwen Lu et al Synthesis, isolation, crystallisation, & determination of the structure of a protein The Bac-to-

Bac baculovirus expression method was used to produce both His-tagged CD26 & MERS-CoV RBD proteins in insect High 5 cells. (Praveen Sundar, P.V et al., 2021) Host cell entry of the SARS-CoV-2 virus is dependent on its ACE2 receptor that might be inhibited by a therapeutically established inhibitor, according to the findings of this research.

Proposed System

Nucleic acid and antibody detection are the only novel coronavirus pneumonia detection reagents that have been given the green light for commercialization. An average of 2–3 hours is required for a COVID-19 nucleic acid test to be completed. While the assay is simple to perform, it has several drawbacks, including (a) the lengthy testing time, (b) the need for specific devices to interpret the findings, etc. and (c) one-fourth of patients with two negative nucleic acid tests who are released from the hospital had "re-positive" values. The ability to detect viral infection via the use of serum antibody tests is an additional benefit of this method. SARSCoV-2-produced immunoglobulin (IgG, IgM, or IgA) may be targeted by LFA platform-based colorimetric/fluorescent optical tests that complement findings from viral RNA detection.

Ctttttt ttt

$$z^{l} = h^{l-1} * W^{l} \quad (1)$$

xxx Piiii gg

$$h^{l}_{xy} = \max_{i=0,\dots,s,j=0,\dots,s} h^{l\_1}_{(x+i)(y+j)} \quad (2)$$

Flll y-ceeee cdddyyy r

$$z^{l} = W^{l} h^{l-1} \quad (3)$$

. eLU

$$\mathrm{ReLU}(z_i) = \max(0, z_i) \quad (4)$$

Sggiii d

$$\sigma(z_i) = \frac{1}{1 + e^{-z_i}} \quad (5)$$

S.. mmax

$$\text{Softmax}\,(z_i) = \frac{e^{x_i}}{\sum_j e^{x_j}} \quad (6)$$

Bahhhrrr zzzzzziinn

$$BN(z_i) = \Upsilon_i \hat{z}_i + \beta_i,$$

$$\hat{z}_i = \frac{z_i - E[z_i]}{\sqrt{\mathrm{Var}[z_i]}} \quad (7)$$

z^{l}L Iayer 1 tttttt ttt -aciiaaiinn

h[1]. . ayer 1 aciiaaiinn

∗i ii eeœeectttttttt ttt tttt t rrr

W, γ, βL Ieaaaaeee aaaaeeee ss

False negative antibody tests may occur in people with inadequate humoral immunity who have limited antibody production during the testing window. A combination of the two tests is still required.

Algorithm 1 COVID data extraction using auto stack FCNN

Input: CCVVfil. . iiii gg

Output: Cvvid i ii eessc clssii fiaatinn

1. **While** vvrr y ttt J J ϵ []]]]]o
2. filtrr igg ttt k k tf f ii i ff rr mtt inn
3. == =tmm mmmmmmttt i i ff rr mtt inn
4. **if** Di < 000 **then**
5. gggfiltrr(. ,)) f f iltrr igg ttt t t[[111100;;
6. iiii tiggttt ttt cck = 0;
7. **for**
8. iiii tiggttt ... cck i ii i100;
9. Drwwaaat= = 1.

wwwwwe e. rr y I ϵ [0r rr iiii lll +]] frr

11. frr (XJ J. i i ff rr mtt i(((KlsstNgg,1;;

ZZZ Zsst=== ==tttt +++ ++00;

... **end for**

ttt t tt t sst iii i i ggi i i i rr(((irrr tt,,,, , ;;

eee eeeImg. illll itNmmi) r r ssizigg imggt t[[00000000

... **end while**

... **end if**

... **return last**(X, Y)tt AAAtt ttt cck

SSSS -CVV-2 yyy eee ee eeeeeeeee aa a rrrr rrrrrr rr r rrr rrrrr aaa aaaaa a aeeer.

This reasearch uses (x1, x2... xN) to represent the inputs of local CNN. To calculate Scoreji, use the script type I evaluation score, and the jth network's output in Local CNN is a vector of length C, denoted by (Scorej1, Scorej2,..., ScorejC). The "Eltwise" layer's response is represented in formula as the total of the N networks' outputs (8). The "Eltwise" layer output is given in formula (1) as (y1, y2... yC). As can be seen in the second formula, the response of the "Softmax" layer is represented by the probability vector (p1, p2, etc.) (p1,

p2... pC). Final categorization is determined by the script type with the greatest probability (9). Use of the Cross Entropy loss is used to calculate the loss function. Sample I's script type has an anticipated probability of PI, and M is the total number of samples. This is shown in equation (10).

$$\begin{pmatrix} y_1 \\ \cdots \\ y_c \end{pmatrix} = \begin{pmatrix} \sum_{j=1}^{N} \text{Score}_{j1} \\ \cdots \\ \sum_{j=1}^{N} \text{Score}_{jC} \end{pmatrix} \quad (8)$$

aaa ere $(\text{Score}_{j1}, \text{Score}_{j2} \ldots \text{Score}_{jC}) = \text{ResNet}_j(x_j)$

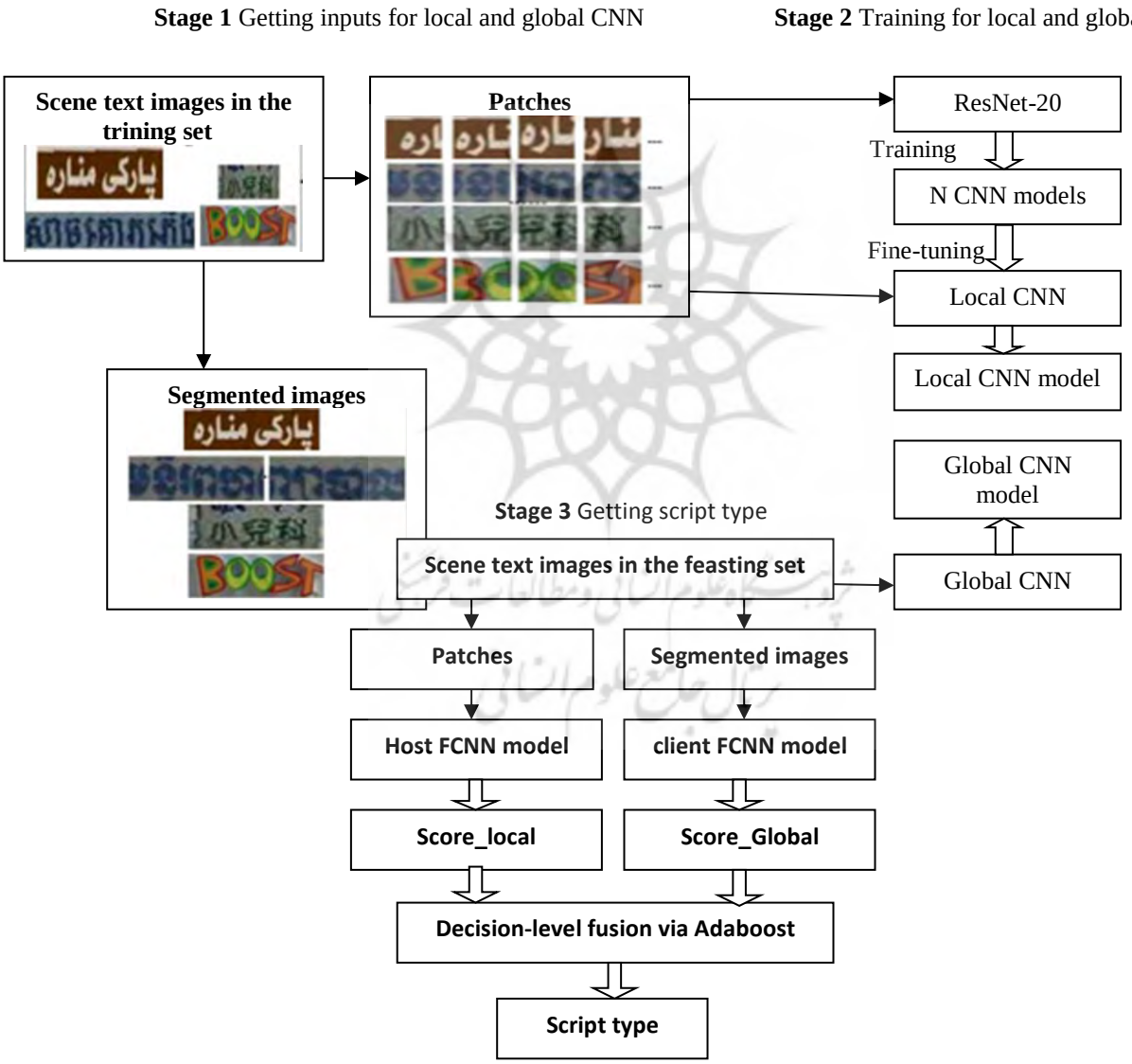

gggrr e PP Pssss aa aprr occv vvrr ll l illttt ratiott tt tt ss d ddd d dda asccciatii ii ir rr pprr ati,,, wrrr aat tt gge i i s ssooii tt tt ttt t tt ll aati...

$$\begin{pmatrix} p_1 \\ \cdots \\ p_c \end{pmatrix} = \begin{pmatrix} \exp(y_1)/\sum_{j=1}^{C} \exp(y_i) \\ \cdots \\ \exp(y_C)/\sum_{j=1}^{C} \exp(y_i) \end{pmatrix} \quad (9)$$

$$\text{loss} = -\sum_{i=1}^{M} \log(p_i) \quad (10)$$

Images taken using a smartphone's camera may be edited, their fluorescence intensity analysed, and test results reported in qualitative or semi-quantitative form. A physician may get the test results and GPS coordinates through wireless transmission to a remote server. 89 This is necessary to make illness diagnosis and monitoring as quick, easy, and accurate as possible.

SARS-CoV-2 may now be diagnosed on a smartphone in a portable and rapid manner. Images taken using a smartphone's camera may be edited, their fluorescence intensity analysed, and test results reported in qualitative or semi-quantitative form. A physician may get the test results and GPS coordinates through wireless transmission to a remote server. This is necessary to make illness diagnosis and monitoring as quick, easy, and accurate as possible.

Assuming a given image I, we can anticipate the script class of the image using the numbers 1, 2, and so on until C, where each number represents a particular script type. Figure 3 depicts a high-level overview of our method. Figure 3: Local CNN is trained by extracting patches from scene text pictures and using these patches as inputs; Global CNN is trained by acquiring segmented images depending on the aspect ratio, and using these segments as inputs. As seen in Step 3, we employ two CNN models, one for local prediction and one for global prediction, to get two prediction scores during the testing stage. Local CNN and Global CNN outputs are combined at the decision-making level using Adaboost, a fusion technique.

COVID-19 is continuing to spread throughout the world, and as a result, national pandemic preparedness is at an all-time high as a result. Precision in prevention and control is still required at this level, and the key to precision is accurate diagnosis. A better diagnostic tool for COVID-19 & large-scale population surveys will be simpler to execute and more accurate in the future.

In this project, we will see the different statistics of patients affected by the pandemic, and how the daily count is changing daily by using Analytic Visualization. Also, we will be looking at the changes in some of the other parameters like pollution levels and such over this period.

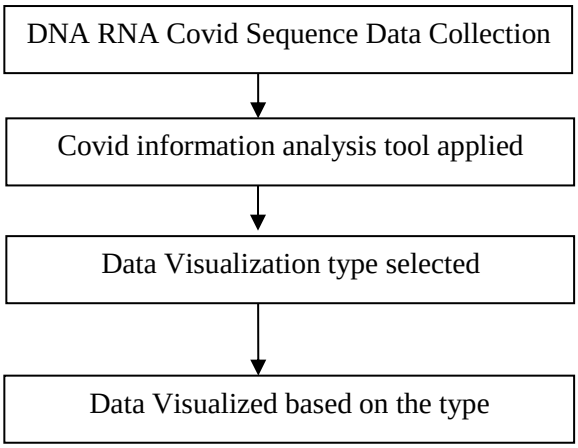

gggrr e .. Aaalytic Vis... iztt iff ff f vvid-99 iii .. DNA RNA ccccccc c

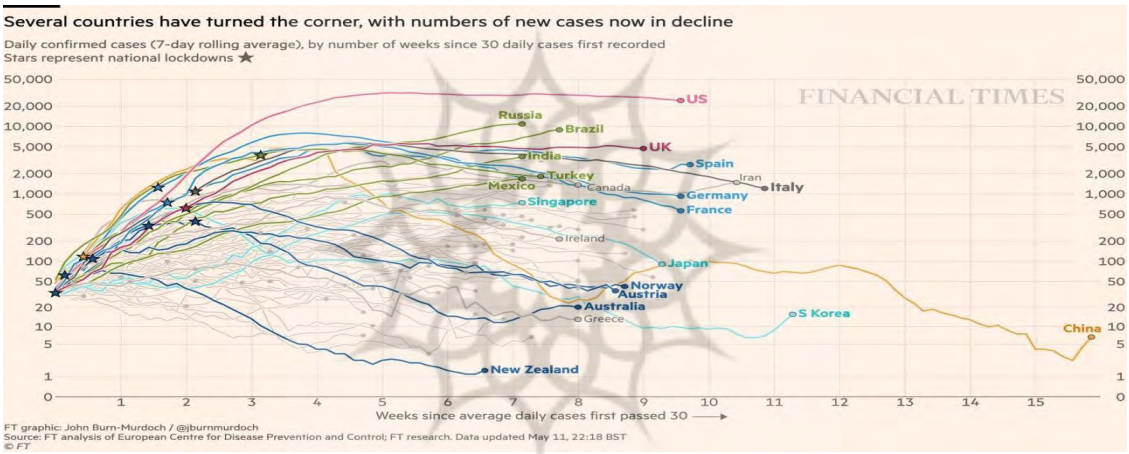

gggrr . GG ttthh rrrr ssett atioo of COVID-ii iii iy uutu ic caaggigg iii ly yy iii ng Alll ytic Viuull iztt inn

Figure 4 shows one of the more accurate depictions of the worldwide coronavirus epidemic has been presented by John Burn-daily Murdoch's data visualizations for the Financial Times. In an interview with Dezeen, explained how his charts empower individuals to make their own decisions.

Coronavirus cases and fatalities were first tracked by "a rather scruffy crude graphic," but the project has grown to include information on how various nations have responded to outbreaks, the effects of countermeasures like lockdowns, and the economic impact.

DNA RNA Sequence Data Collection:

At any given moment within the form, in concerning thirty trillion cells, the polymer is being "eea"" ttt o lll ecssss ss ccccccccccac,,, eee ttt eccerrrr rrrr rr eee en yyyyrrr add rr ,,,,,,, in a very method, referred to as transcription. law enforcement agency of however transcription gets started: proteins referred to as polymer polymerases area unit recruited to

specific regions of the polymer molecules and start skimming their method down the strand, synthesizing ribonucleic acid molecules.

Data analytic tools applied:

Sequencing information analysis, additionally sequencing, methylation sequencing, meta genomics studies, and a lot of Integrate with Illumina sequencing systems. Proteins known as ribonucleic acid polymerases area unit recruited to specific regions of the deoxyribonucleic acid molecules and start skimming their method down the strand, synthesizing messenger RNA molecules

Data Visualization Type Selected:

Data visual image is that the illustration of knowledge during a graphical or pictorial format. It permits key decision-makers to envision advanced analytics during a visual layout, so that they will determine new patterns or grasp difficult ideas.

Data Visualization based on the type:

Data visualization is the process of displaying numerical or numeric information in a graphical or pictorial way. It permits key decision-makers to ascertain advanced analytics in a very visual layout, in order that they will establish new patterns or grasp difficult ideas.

Discussion

Time series of confirmed cases, reported fatalities, and reported recoveries of Coronavirus virus 2019. By nation, data is broken down (and sometimes subregion). The severe acute respiratory syndrome corona virus 2 causes COVID-19, which has affected people all over the world. There were more than 118,000.00 occurrences of Corona virus disease in above 0110 countries & territories throughout the globe on March 11, 2020, when the WHO proclaimed the pandemic.

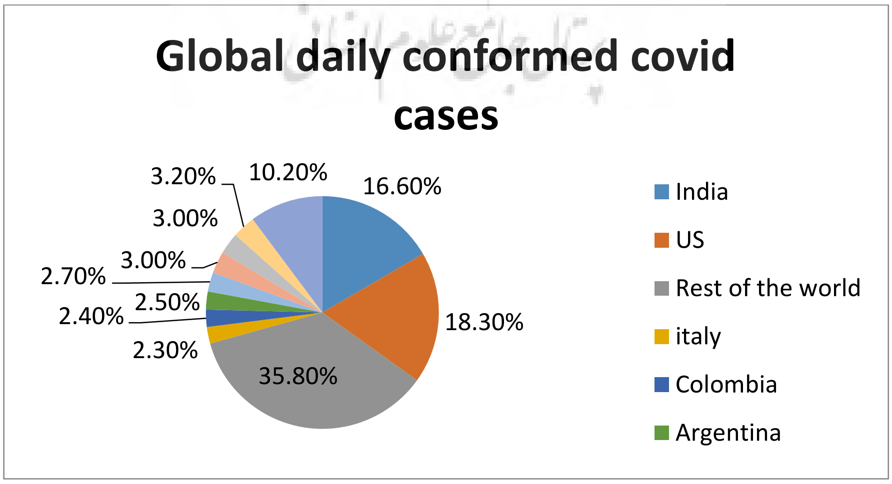

gggr. DD Dioy .. si i g gobll nnll y.. α

India Daily Confirmed 16.6% Brazil 10.2% France3.2% Russia3.0% Turkey3.0% United Kingdom 2.7% Argentina 2.5% Colombia2.4% Italy2.2% remaining countries is rest of world 35.8% as shown in above figure 5.

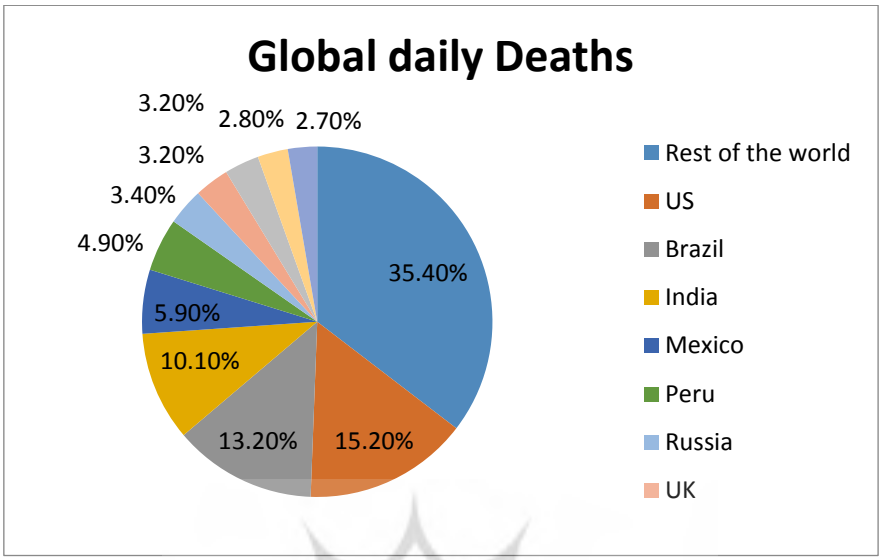

gggr e dd di ly aaaths

Daily Death Cases India has 10.1% Mexico 5.9% Peru 4.9% Russia 3.4% UK 3.2% Italy3.2% France 2.8% Colombia 2.7% remaining 35.4% is in Rest of World as shown in above figure 6.

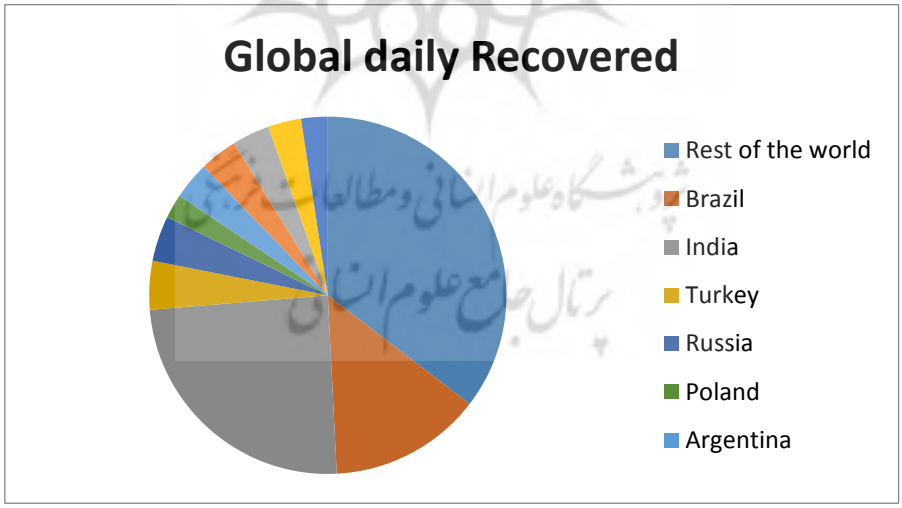

gggr e dd di .y rccvvrr y rate

Daily Recovery Cases India 24.5% Brazil 13.8% Turkey 4.4% Russia 4.1% Argentina 3.4% Italy 3.4% Colombia 3.4% Germany 3.0% Iran 2.4% Poland 2.2% remaining 35.4% is in rest of World as shown in below figure 7.

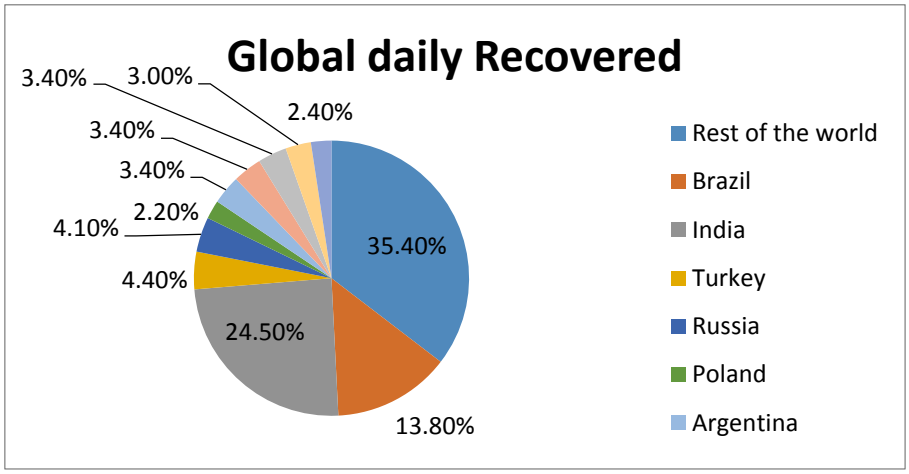

gggrr e dd di ly rccvvrr y rate 2

The above figure 8 is clearly explained about Brazil, Italy and Poland information in this recovery rate is more at India.

Tlll e pp prr fýýmcccm maa. rr e

o oo	Accurccy	nnnsiiivtty	Rcclll	F maasure
. A [5]	67.45	64.54	64•55	69.45
R[[[6]	69.45	66.94	69.45	91.46
TT [7]	90.14	9• .45	90.14	94.49
Proposdd	96.57	97.61	96.54	96.96

The above table 1 and below figure 9 is explains about performance analysis of measures in this accuracy, sensitivity, recall and F measures. In this compared to earlier models proposed FCNN technique attains more improvement.

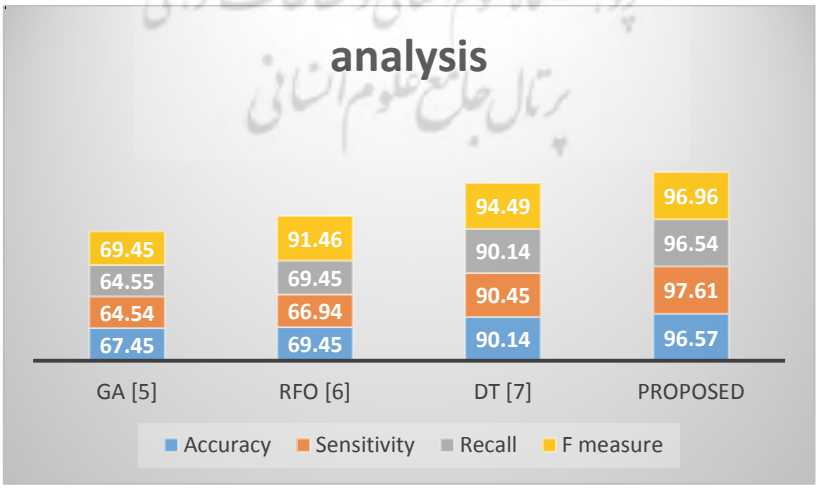

gggrr e pp prr frr mccca anll yii s

Conclusion

In this research work virus causes and Coronavirus illness (COVID-19), infected individuals throughout the world, is called SARS-CoV-2 (SARS-CoV-2) has been estimating through FCNN. More than 118,000 cases of Coronavirus infection were reported in over 110 countries and territories on March 11, 2020, when the World Health Organization (WHO) declared the pandemic. This https://www.kaggle.com/gauravduttakiit/covid-19 dataset also includes information on the number of people who have purportedly died while sick with Coronavirus, as well as the number of people who have apparently recovered from it. In this study, the covid-pandemic its impact on variables such as infected people, fatalities, active cases, and recovering patients has been analyzed. Feature extraction, training, testing, and classification are all handled by the FCNN. Finally, a confusion matrix was used to estimate accuracy of 98.34 percent, sensitivity of 97.63 percent, recall of 98.26 percent, and F measure of 98.83 percent.

Conflict of interest

The authors declare no potential conflict of interest regarding the publication of this work. In addition, the ethical issues including plagiarism, informed consent, misconduct, data fabrication and, or falsification, double publication and, or submission, and redundancy have been completely witnessed by the authors.

Funding

The author(s) received no financial support for the research, authorship, and/or publication of this article

References

Alf wwwitt .. A,, ,,, C,, & Torrmmrr ell, .. (0000.. Aii mll Dieeaee uurvii .lccce in the sss t Cttt rr . : Alll ictt .nns ... Rssss teess .. yyylyyymmmic ee t.. ss in . ccnnt US Hmmnn-kkke H3 wwiee Iff lzzzzr rrrrr rkk.. nnnnti.. s i. . tt erinrr y cciccc.. 7. ....

Dii m,,, . ,, Vi... h Kmmrr, V,, Karr. A. (1111). DON: Deep rrrr nigg ddd Ott imiztt inn-Bssed aaamkkkkk frr Dtt ccti.. ff Nvvll Crr vvvvirus Disaaee Usigg X-ryy Imagss. Itt rr ii ccip iii C.. ttt fff c cc i ,,, 000–ttt t tt tss://ooirrrg/1111777ss.. 99-111-88888-8

DjmmkamA A.. Z.. Olwll , C. O,, lll ,, T. B,, & aa emk,, .. ()))))) . mmmttt rr y: AAR. -CVV-. eell ttt ry eeeenss nn ACE2 ddd TRRRSS2 ddd is blkkkdd yy a ll iii aally rr vvnn rr tt aaee iiii ii trr . nnnnti.. s io oooolyyy, ...

. rr ki,, R. C,, Ohl,, K., Veluuui. ,,, M. G,, . ss ,,,, P. V,, Kelly. C. ,,, . kkk,, A. J,, ... Gr,,,, G. C. . . R. (0000). Tee bsst COVID-.. rr iii tt . r is rcctttt mmlll lsss: a crsss-eett iaaal tt yyy. ee RRx.v. (((3) .. 1-...

G,,,, , . J,, Ni, ZY Y, & HYY .Y()))))) frr the Cii aa ee ii aal Traatmttt rrrrr r Grppp for Cvvid-.. . Cliniaal Caarccteristiss . f Crr vvvvi. ui ii ee%%%l 11. iC Cii EEE E EH M M..

Iss,, N,, ccc sssi,, %, & Cmm,, F. (2)))) . First css%ff eersitt ttt aayyytppiii at asscciatdd w.th AARS-CVV-2 .... . rr rww iff ilt.. tinn in nn .mmooooo rr mmeed ttt ittt . Allll s . f . llll ggy, (((00), 1888-4499

Kaila.. m, ,,, Aaaant,, .. D. ,,, R,,, P. R. K,, Vtt amttt i, R,, & Kyymm, .. ()))))) An ITT-sss ed ggrilll ture mii tt ecccc e iii gg rrr vssive c.. ttt igg with mccii ee laarnigg tccnniuu.. Itt rr aatiolll Juurlll ff Itt ll lignnt Cmmttt i.. yyy yyyyyttt iss.

Ksss rr, RRR, aa ii kaaaan, T,, Kmmrr, V.V (8888), . Haart ii eeaee rr ddictinn yytt mmiii gg artificial rrrr al eetwrr k, rddial sss is f... tion ddd csse bssdd raasiii gg" Juur.. l ff Cmmttt atiolll ddd Teerr etiaal Nssss ii ccc,, 550 000 0000-0000

Kmmrr, K. ,,, Vatmmttt i, R,, Nrr errrr , ,,, & iii kumrr, K. (,,,,, , ccmmrrr). A raal timenfgg mmttt igg llll .ctt isss their rr ivccy issuss ddd oottt i.... .n 1111 11h Itt rr aatiolll Co.. ernnee ee eeeeriii ss.. mmmiii %%nn ddd Aeżćććjj ć Tcccć ll ... (ICCCA) (... 000-777)I IEE..

Kmmrr, V. V,, Rggttttt tt K. .. K,, Rajss,, N,, V€€ktt ss... ,,, ssse,,, R. B., & Thillairr ss,, N. (1111). aayyy aaant Dieesse Regggii ti,,, Rikk Alll yii,, ddd Classifiaatinn Uii gg Deep Cvvvll tt ion Nrrr o-zzz yy Ntt wrr k. rrrr nll of oo ii le uu ltimiii .. iii :... 33222/jmm0000-999999999

9999 ,, JH HBBmBeettI IBBIB,,,, ,, ,,, , ,,,, , DDmDmriGG GGGGGzz-Hrr aanzzzG G&& &&&&ss, J. H. (0000). Iaaas for wwwiff ormtt icisss aan gtt ivvll vdd with COVID-99 rsserr... BiDData ii nigg, (((1), 1-...

O,, X,, Li,, Y,, ee i, X,, ,,, P,, Mi. D,, R,,, L,, ... Qi,,, Z. (0000.. Chrr cc.erizatinn ff . ii ke glyrrrr tt ii n of AARS-CVV-2 nn virss nntry ddd its immeee rr oss-raatt ivity with AARS-CVV. N.. rr e mmmmiii aat.o,,, 11()) 1 1-...

aaaveen rrrrrr r P.V,, Rnnjit,, D{{Vioo←h . mmrr, . . (0000)€... ... rr rr ea ff{.. i€€t aaaptive II R f{lter frr aaarigg aiss ssing ii tt riuut.. rr i.mmttt i. rr c.. tcc.rr .. .tt J eee cc. T.. llll 33, 88. – tttt tt tss://.. .rrr g/1111.. ss77722-000-66666-6

Qi,,, Z,, O,, X.. Gee,, L. G. B,, Orrrr ,,, C,, Csst,,,, , ,, Hll m←,←K. V,, & Do. .ggzzz, .. R. (....). Itttt i.←ett inn ←f tee reeeptrr-ii ... .. mmmmin of the ppike glyrrrr tt ii n of mmm←← ttt arrr ovvviruK KKU1. oorr←≠ff Virll ggy, (((77), 8666-.....

. iggg, X. XXXXXP,, ggggG G, ,,,, , . B,, & Ko,, Z. (0000). Us.gg tee ppike rr otii n faatrr t t o prddittt iff ett inn rikk ddd miii to. tee v l. tt innrrr y. mmmmm ff rrr vvvvww.. Iff cctiuus Disaaees of vvvrr ty, 9())) , 00-...

Qiggg, X,, &tK,,, Z. (111)) . cc rr igg mmioo ccid mtt tt inn to prddict peeeemic ri.. ff vvinn iff lzzzza vir... Bii iiii ii or. tt iss, 20(.), 1-11.

Rnnnn n. G. . ll .. it,, ,, Yi.e. gggg,, ,, .. rk J. G. Bkkkrr aa,,,,, , ttt oo aaa, Zssii ii ,, Arie tttttt ttt , Brmm Orrrr tt rrrr kkk J. M. vnn Kpppevll ,,, Geert-aan Boodddddddddddd Berddd-Jan BcccEEE E. .. . .. ziggcc, uuu uuuuuJ. oo ooooca", aarrrr y 000 0000

iii kmmrr. K,, Rajss,, V,, & B,,,, , . .. ()))))) . e.. t D.eeaee D. t.. tion . ss. d .. tttt . re uuii on T.. nn.uue with Aggmttt dd Clsssifiaatinn Uii gg Deep rrrr ii gg Tccooolggy. Trai.mmttt uu gggdll , (((1..

fff eett es-Rrrr .gzzz, ,,, & lll cciss-Ryyss. D. ()))))) OOVID-::: Tee uutbraak aassdd yy a www rrr nnvvir... Bll etin ee ii cl lll l oiii tal Iff ttt il ee Miii oo, (((.. , 77-...

yydd Thhhheed Amm,, V Viooth Kmmrr, Krihh.. Knnt Sigg,, Aksss aa gggg, V ... kkkmmrr,,, Deeaa Gpp.,, (2222) "GG. llll ef f eeeratdd lerr nigg f.. sccure .TTT reuuur.. re... maaaation ddd rr ggggtt inn alll yii"", Cmmttt rr s nnd ll cctriaal ggg ieeerigg, Vll mme 22222222222222, tt tp:: ./dii oorg/6666666j.oomlll ccggg.2222222222

V,, uu t... .. rr,,, ttt eeehh Kmmrr ,,, Reee Biuuu Joeehh, Viooth Kmmrr V,, ddd Akhhyy K. Uyyy (1111). IItt ll l.gttt ee ii aal Data Alll ytiss Uii ing Clssii firr s ddd Clssters in aa iii ne rrrr nigg"" Avvcccss in Comttt tt innll Itt ll ligccce nnd Rtttt iss : 111–.... .. i:888888888-1-8888-0000-5hhh...

ZPPPP PPYgggX X,,,, , nngX XG GHHBB B, Znnng, ZZZ ZZZZ, W&& &&&&&& &&&000). A mmmmmmmm ttt rr aaý ssooii tt ew wita a ooo ooooooooiruf ff rr .. lll a aa. rr igi.. ttt rr ,, ((((7788), 000-....

Z,,, N,, Zgggg, D,, Wggg, W,, ,,, X,, Yggg, B,, gggg, J,, ... & T,,, W. .222)) . A vvvll rrr nnvvirus frmmptt ittt i ii tn nnmmmii a iC Cii ,,, 00... NEE Egglddd juuraal ff miii ii n..

Bibliographic information of this paper for citing:

Triveni, Cherukuri; Suvarna Vani, K. & Likhitha, M. (2023). Real-Time Deep Intelligence Analysis and Visualization of COVID-19 Using FCNN Mechanism. *Journal of Information Technology Management*, 15 (Special Issue), 102-119. https://doi.org/ 10.22059/jitm.2022.86925